Available online at www.sciencedirect.com
SCIENCE DIRECT
International Journal of Mass Spectrometry 253 (2006) 263–273
International Journal of Mass Spectrometry
www.elsevier.com/locate/ijms

Probing solution- and gas-phase structures of Trp-cage cations by chiral substitution and spectroscopic techniques

Christopher M. Adams [a,*], Frank Kjeldsen [a], Alexandra Patriksson [b], David van der Spoel [b], Astrid Gräslund [c], Evangelos Papadopoulos [c], Roman A. Zubarev [a]

[a] *Laboratory for Biological and Medical Mass Spectrometry, Uppsala University, Box 583, SE-75123 Uppsala, Sweden*
[b] *Institute for Cell and Molecular Biology, Division of Molecular BioPhysics, Uppsala University, Sweden*
[c] *Department of Biochemistry and Biophysics, Arrhenius Laboratories, Stockholm University, Sweden*

Received 16 February 2006; received in revised form 13 April 2006; accepted 25 April 2006

Abstract

The relevance of gas-phase protein structure to its solution structure is of the utmost importance in studying biomolecules by mass spectrometry. D-Amino acid substitutions within a minimal protein, Trp-cage, were used to correlate solution-phase properties as measured by circular dichroism with solution/gas-phase conformational features of protein cations probed via charge state distribution (CSD) in electrospray ionization, and gas-phase features revealed by tandem mass spectrometry (MS/MS). The gas-phase features were additionally supported by force-field molecular dynamics simulations. CD data showed that almost any single-residue D-substitution destroys the most prominent CD feature of the "native" all-L isomer, α-helicity. CSD was able to qualitatively assess the degree of compactness of solution-phase molecular structures. CSD results were consistent with the all-L form being the most compact in solution among all studied stereoisomers except for the D-Asn^1 isomer. D-substitutions of the aromatic Y^3, W^6 and Q^5 residues generated the largest deviations in CSD data among single amino acid substitutions, consistent with the critical role of these residues in Trp-cage stability. Electron capture dissociation of the stereoisomer dications gave an indication that some gas-phase structural features of Trp-cage are similar to those in solution. This result is supported by MDS data on five of the studied stereoisomer dications in the gas-phase. The MDS-derived minimum-energy structures possessed more extensive hydrogen bonding than the solution-phase structure of the native form, deviating from the latter by 3–4 Å and were not 'inside-out' compared to native structures. MDS data could be correlated with CD data and even with ECD results, which aided in providing a long-range structural constraint for MDS. The overall conclusion is the general resemblance, despite the difference on the detailed level, of the preferred structures in both phases for the mini protein Trp-cage.

Keywords: Solution structure; Gas-phase structure; Chirality; Electron capture dissociation; Charge state distribution

1. Introduction

The structure of polypeptides is fundamental to all aspects of biology. Solving protein gas-phase structures will help us to better understand the laws governing formation of secondary and tertiary structures of these molecules, and the role of water in assisting the formation of protein conformations. Mass spectrometric structural studies on biomolecules involve a solution-to-vacuum transfer. The solution structure can be studied by an array of well-established techniques including crystallography, nuclear magnetic resonance (NMR), differential scanning calorimetry (DSC), RAMAN spectroscopy, and circular dichroism (CD). All of these techniques have inherent advantages and disadvantages [1]. CD is a formidable solution-phase method for the investigation of secondary and tertiary structure as it is non-destructive, offers relatively good sensitivity compared to other solution-phase spectroscopic techniques and allows for the same sample to be measured at various temperatures [2]. The far UV region (wavelengths between 185 and 250 nm) are exploited to provide signature secondary structural signals [3]. The near UV (250–550 nm) provides hints to the structural assembly of the aromatic side chains of Trp, Tyr and Phe and is commonly used as a qualitative measure for tertiary structure [4].

In the gas-phase, polypeptide structures can be probed by a variety of techniques based on electrospray ionization [5] and mass spectrometry (MS) [6], ion mobility MS (IMS) [7] or

* Corresponding author. Tel.: +46 18 471 5729.
E-mail address: chris.adams@bmms.uu.se (C.M. Adams).

1387-3806/$ – see front matter © 2006 Published by Elsevier B.V.
doi:10.1016/j.ijms.2006.04.012

tandem MS (MS/MS). Gas-phase analysis performed by MS is much more sensitive than conventional structure determination with NMR and X-ray crystallography. However, the link between the solution structural features of polypeptides on one hand and their gas-phase behavior on the other hand is not well established. While many studies on specific systems concluded that gas-phase structures may be similar to solution structures under certain, well-controlled conditions [7–9], there are a number of other studies indicating large divergences [10,11].

The transition to the gas-phase occurs during the electrospray ionization process [5], which by itself is not completely understood [11]. After two decades of studies and debate, the aggregate evidence suggests that the charged residue mechanism dominates for larger polypeptides [12]. This mechanism postulates successive droplet fission followed by complete solvent evaporation from the smallest droplet before the emergence of a "naked" multiply charged gas-phase ion. An interesting question is whether the charge state distribution (CSD) of these ions observed in ESI reflects more the solution-phase structure or the gas-phase structure. While some studies implicitly assume the first alternative [13], one of the few existing quantitative models operates with gas-phase basicities of amino acid residues [14].

Generally speaking, changing the solvent environment to that of vacuum promotes more extensive hydrogen bonding and drastically decreases hydrophobic interactions, while coulombic forces between electrical charges increase. Thus the protein structure almost certainly undergoes noticeable changes. But as such, the process of drying can preserve certain structural features. The question is whether the same applies at the molecular level. One school of thought maintains that gas-phase proteins likely retain some common similarities with the native solution-phase structure [7,15,16]. One of the alternative views is that of the "inside-out" conformation [17,18], according to which upon leaving the solution-phase polypeptides undergo such drastic structural changes that their gas-phase structure bears little resemblance with the original, "native" conformation.

This view, unsupported at the macroscopic level, is based on the peculiarity of the structure of many soluble proteins that have a core of hydrophobic residues surrounded by layer of solvent-exposed hydrophilic ones. The hypothesis states that in the absence of solvent the reverse should be true as polar residues would attempt to cluster together for the purpose of internal charge solvation. The same might be expected in a hydrophobic environment, e.g., membranes. However, membrane proteins do not have inside-out structures [19]. The vacuum environment is even more hydrophobic than the membrane, and it increases all electrostatic interactions, including the propensity for intramolecular charge solvation. Thus an inside-out configuration may be hypothesized to arise following the transition from the solution to the gas-phase, which requires a stage of unfolding and refolding. Since the evidence for such unfolding–refolding process can be found in literature for some proteins [10,11,20], the debate moves to a platform of individual cases.

Our interest to Trp-cage (NLYIQWLKDGGPSSGRPPPS) is determined by being a minimal protein used in many studies, both theoretical and experimental, as a test molecule [21–24]. Trp-cage is one of the fastest folding proteins; it obtains its compact shape on a microsecond time scale [23]. Trp-cage is an ideal candidate for studying the solution versus gas-phase relationship, as the molecule is well characterized and is small enough for solid-phase synthesis as well as MDS. To compare the solution- and gas-phase structures of Trp-cage we turn to spectroscopic methods, such as CD, mass spectrometry (MS), and theoretical methods, e.g., molecular dynamics simulations (MDS). Of the gas-phase parameters that MS can probe, the charge state distribution of protein ions in ESI has long been recognized among those retaining the most memory of the solvated state. CSD has been used as a measure of protein folding, with lower charging representing a more folded state [8,16,25]. Although no detailed theory exists that can predict CSD, there have been successful attempts to account for its average value for folded proteins in various electrospray liquids [26].

In contrast to ESI, tandem MS is by definition a destructive method and thus is least expected to preserve intact solution-phase structures. But structural unfolding may not be the same in all MS/MS techniques. While conventional collision-activated dissociation (CAD) [27–29] destroys backbone bond cleavages, secondary and higher-order weakly bound structures [30] and scrambles labile protons [31], the more recent electron capture dissociation (ECD) can preserve weak bonding [32,33]. In a previous communication we have shown that certain features of solution-phase structure of Trp-cage find their reflection in ECD mass spectra [13]. The p*I* value of the Trp-cage is 9.4 and at physiological pH ≈ 7 it has a 1+ net charge. In ESI mass spectra, the charge states 2+ and 3+ are dominant, with their ratio depending upon the solvent, the pH value, temperature, and other experimental parameters. Tandem MS has shown that 3+ Trp-cage ions are fully denatured due to coulombic repulsion between the charges, and that 2+ molecular ions show some secondary and tertiary properties in the gas-phase [13,24].

In order to modulate the stability of Trp-cage cations in solution as well as the gas-phase, we mutated some of the amino acids to their stereoisomeric counterparts. Previously, the ECD fragmentation patterns of "native" and mutated dications were compared for D-Tyr^3 and D-$K^8S^{13}S^{14}$ Trp-cage analogues. In solution (as now confirmed by CD), both mutants lose their stable native configuration and were presumed to do the same in the gas-phase. Subsequently, CAD revealed no qualitative changes in the fragmentation pattern as others have seen with ubiquitin and other peptides [34,35], while ECD gave more extensive fragmentation for D-Tyr^3 and much more extensive for D-$K^8S^{13}S^{14}$ than for the all-L isomer, indicating a qualitative link between the degree of unfolding and ECD pattern. In a more recent study, dications of four stereoisomers (all-L, D-Tyr^3, D-Gln^5 and D-Leu^7) were fragmented by ECD and their gas-phase structures simulated by force-field MDS to reveal the ECD–structure correlation and deduce the ECD mechanism [36]. Here we investigate the *quantitative* relationship between the structural features in two phases by studying the solution structural features by CD on nine Trp-cage stereoisomers, including mutants with a single L → D substitution of each of the first seven N-terminal amino acid residues. To reduce the error arising due to varying experimental conditions, relative measurements were performed. For this purpose, an all-L Trp-cage was synthesized with all three

glycine residues deuterated, and this +6 Da heavier molecule was admixed to other stereoisomers and used as an internal standard. To study the effects of solvent, different electrospray conditions were tested and two of them were used for quantification studies, 2 mM ammonium bicarbonate, a buffer used in many studies to promote "native" structure formation [37,38], and 100 μM quinhydrone (Q), a redox reagent effectively diminishing the average charge state of electrosprayed proteins [39].

2. Results

2.1. Solution structures by circular dichroism

Solutions of all nine Trp-cage stereoisomers were studied by CD using the far UV region to reveal the extent of folding, particularly α-helicity. CD measurements were taken at 10 °C intervals from 5 to 65 °C, but for reasons of clarity only three temperatures (5, 25 and 65 °C) are shown in Fig. 1A. In all cases, the lowest temperature showed the highest structural content. Alpha-helix was still present in the first two D-substituted stereoisomers (D-*Asn*^{1}, D-*Leu*^{2}) as well as in the deuterated native form. Correlation analysis was performed between the data points taken between the wavelengths of 190–205 nm (region of the most prominent signal for an α-helix) for a stereoisomer on the one hand and the native form on the other hand. Not surprisingly, the analysis showed the highest correlation ($r = 0.999$) for the deuterated native form. The other two stereoisomers, D-*Asn*^{1} and D-*Leu*^{2}, produced $r = 0.995$ each, indicating the comparatively small importance of the chirality of first two N-terminal residues in the α-helix. At the same time, L → D conversion at the aromatic residue Y^3 destabilized the α-helical portion of Trp-cage ($r = 0.915$) as well as the tertiary structure (Fig. 1C). Interestingly, chiral substitutions at *Leu*^{7} ($r = 0.853$) as well as at $K^8S^{13}S^{14}$ ($r = 0.868$) gave rise to a distinctive 3_1-helix signal, which in the all-L solution structure is much less prominent than the α-helix and spans from residues 11 through 14.

Ellipticity at 222 nm (Fig. 1B) is traditionally used in CD to monitor the degree of α-helix content as a function of temperature. In Fig. 1B, three secondary structural classes can be distinguished. Trp-cage, deuterated Trp-cage, D-*Asn*^{1} and D-*Leu*^{2} all produced a positive a slope, signifying α-helix content. The native form displayed the highest degree of helicity content and mirrored previously published CD data very well. The second structure, random coil, occurs after D-substitutions made at position three through six and show no slope in Fig. 1B. 3_1-Helix (a structure not especially prominent in CD) is exhibited by D-*Leu*^{7} and D-$K^8S^{13}S^{14}$ isomers, which show the only two negative slopes at 222 nm.

The somewhat surprising difference in the slopes produced by the native and deuterated forms of the all-L isomer can be explained by the lower concentration of the deuterated form and admixture to it of truncated peptides. The presence of a small amount of the latter species was confirmed by mass spectrometry. This however did not cause any obstacles for CSD and MS/MS measurements, where only correct molecular masses where taken into account (CSD) or selected for fragmentation (MS/MS).

Circular dichroism is also useful in the detection and monitoring of tertiary structure, specifically analyzing the near UV region of the aromatic residues Trp, Tyr and Phe. As such we show in Fig. 1C the near UV spectra of all-L form and D-*Tyr*^{3}, indicating the presence and absence, respectively, of compact ternary structure. Near UV studies require substantially more concentrated samples, and therefore we limited our studies to the all-L, deuterated all-L and D-*Tyr*^{3} stereosisomers. These data conclude that a single D-amino acid substitution does disrupt the tertiary structure and the deuterated all-L still retains its structure in solution.

2.2. Charge state distribution in mass spectrometry

CSD is easily monitored on the same mass spectrometer that is used for ECD, which reduces errors due to the instrumental factors. Three CSD parameters were quantified. The first parameter was the average charge state (ACS) determined as

$$\mathrm{ACS} = \frac{\Sigma\, N_i I_i}{\Sigma\ I_i}$$

where N_i is the charge state of the intact molecule and I_i is the relative abundance of all peaks in the isotopic cluster of that charge state. For every stereoisomer, the difference ΔACS with the admixed deuterated all-L internal standard was determined. To quantify the *relative* size of the effect of L → D substitution on ACS, the parameter γ was introduced and defined as

$$\gamma = \left(\frac{i_3}{i_3 + i_2}\right) - \left(\frac{i_{3\mathrm{H}}}{i_{3\mathrm{H}} + i_{2\mathrm{H}}}\right)$$

where i_2, $i_{2\mathrm{H}}$ and i_3, $i_{3\mathrm{H}}$ are the sums of the intensities of 2+ and 3+ molecular ions normalized by their respective charge to account for the difference in the detection efficiency in an FT-ICR mass spectrometer. The nomenclature i describes the sample protein (all-L or D-substituted) and subscript H (heavy) denotes the deuterated all-L form.

Fig. 2A and B shows partial mass spectra of Trp-cage 2+ and 3+ ions in AB and Q solvents, respectively. The higher mass ions represent in all cases the deuterated all-L Trp-cage used as an internal standard. The ACS, ΔACS and γ values are shown on the figures as well. As a control, light and heavy variants of the all-L form showed close ACS values for both buffers, and revealed the error of γ measurements (±0.02). Additionally, to provide a tight experimental error measurement 45 individual CSD experiments of the deuterated all-L Trp-cage were analyzed. Twenty-seven independent experiments using ammonium bicarbonate and 18 experiments using Quinhydrone revealed a standard error of 0.022 and 0.026, respectively. In effect all ΔACS values and γ values greater than their experimental error in respective solutions are considered to be conformational deviants. The γ values above zero indicate that the ACS of a stereoisomer is higher than that of the standard, and that the stereoisomer is more basic or has a contrasting surface area in solution than the native form [40]. Since L → D substitution does not change the chemical reactivity of amino acid residues, the reason for the increased average charge state is the less compact conformation as observed in the CD data shown in Fig. 1A. All

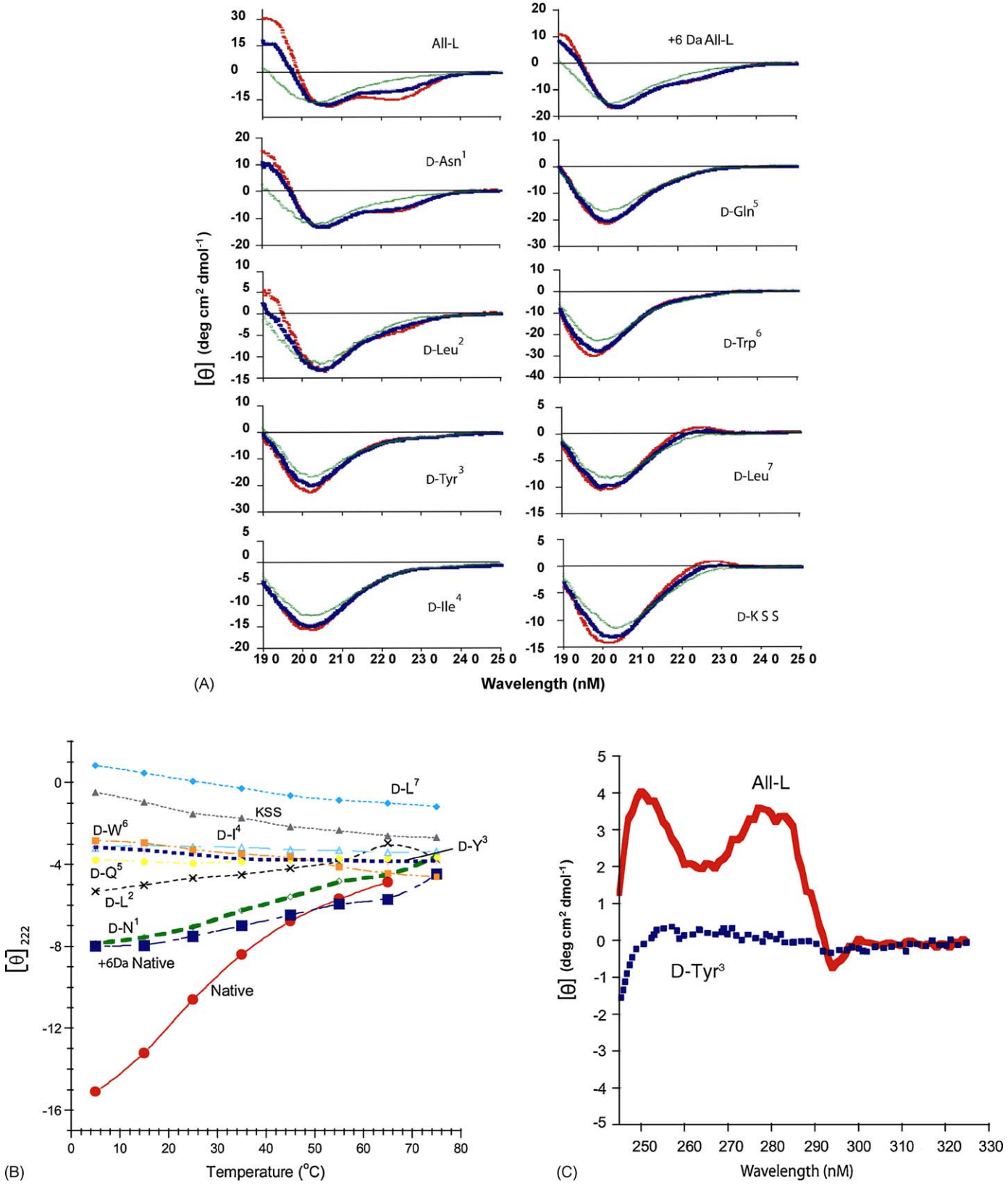

Fig. 1. (A) Circular dichroism data at wavelengths 190 to 250 nm. Eight temperatures were monitored but for reasons of clarity three are shown, red 5 °C, dark blue 25 °C and light blue 65 °C. (B) Circular dichroism elpicity (θ) melt at 222 nm, a common indicator of α-helix. D-Amino acid substitutions are indicated; +6 Da represents the deuterated form of the all-L isomer. C) Near UV spectra of all-L Trp-cage (solid line) and D-*Tyr*^{3} (dotted line) showing the aromatic response, or lack thereof for *Tyr*^{3} and *Trp*^{6} residues.

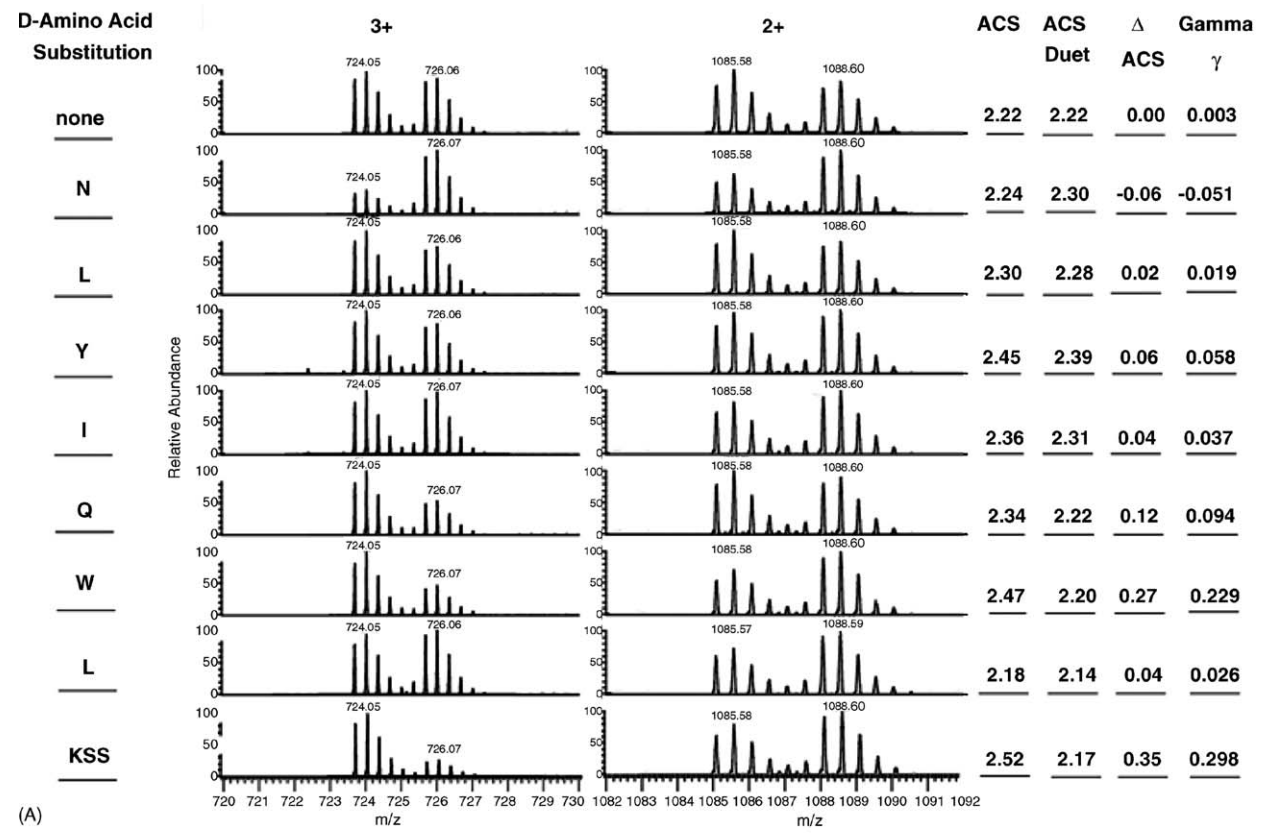

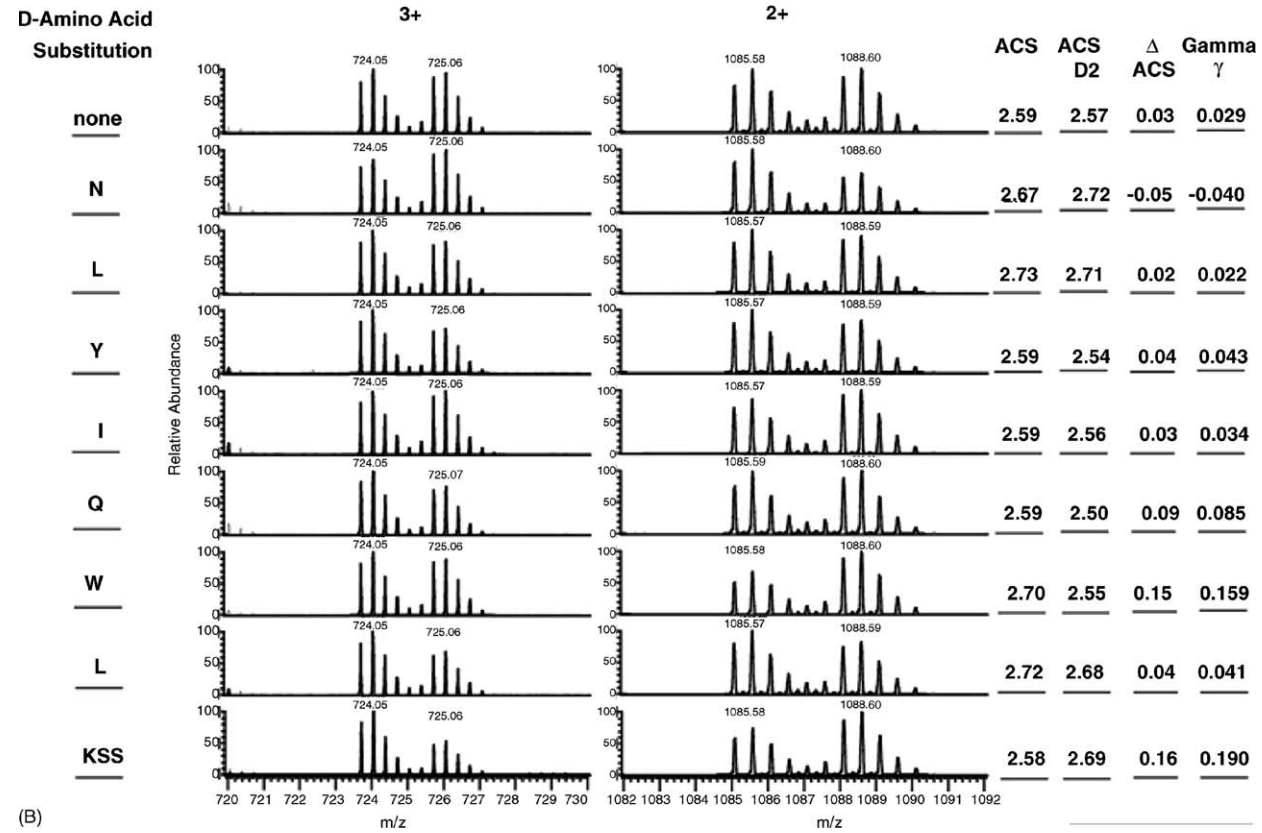

Fig. 2. Charge state distributions of mixtures of deuterated (+6 Da) native and series of D-substituted stereoisomers in (A) 2 mM ammonium bicarbonate and (B) 100 μM quinhydrone solutions. ΔACS is the difference between the average charge states of the D-substituted and deuterated native isomers, and γ is a relative value of the charge state shift.

stereoisomers except D-*Asn*[1] show $\gamma > 0$, consistent with the all-L Trp-cage being the most compact form of the protein in solution. The result for D-*Asn*[1], for which $\gamma < 0$ for both solvents, may be due to the fact that the minimization of Trp-cage has been performed by amino acid substitution [22], but not L → D mutation, leaving free the possibility of further optimization by this degree of freedom. The solution-phase structure of the D-N^1 mutant is currently under investigation by NMR, which unlike CD provides a full tertiary landscape of backbone and side chain contacts.

The γ data were quantitatively similar for both solvents, despite the significant variation in ACS values. Of single-substituted stereoisomers, D-*Trp*[6], D-*Tyr*[3] and D-*Gln*[5] mutants were the most unfolded. The effect was fully consistent with the critical role these residues (particularly the tryptophan) play in the Trp-cage structural stability [41]. Multiple D-$K^8S^{13}S^{14}$ substitution produced the strongest overall effect on γ, in parallel with the gas-phase data from the previous study [13]. Generally, the position of the amino acid in the sequence played a critical role as such that D-substitution in amino acids closer to the N-terminus produced a smaller destabilizing effect. In summary, the above results indicate the potential of CSD for probing the effect of the most-subtle structural changes on the solution structure.

2.3. Structure analysis by tandem mass spectrometry

The gas-phase properties were tested on the charge state 2+ for each stereoisomer, because earlier results proved that this charge state is most likely to preserve the solution-phase properties [13,24]. Three gas-phase parameters were measured: (i) stability of the charge-reduced species, λ; (ii) relative deviation of the ECD pattern from that of the native Trp-cage, α; and (iii) relative spread of the ECD fragment abundances, β. The meaning of these parameters is given below.

Fig. 3 shows the ECD mass spectra of 2+ molecular ions of stereoisomer mixtures electrosprayed from quinhydrone solution. In all cases the product ions were singly charged, C-terminal $z_{15–19}$ fragments, as well as the charge-reduced molecular species $[M + 2H]^{+\bullet}$. For D-substituted molecules, the z-ion abundances were normalized by the abundances of the same ion from the admixed internal standard. The abundances of the charge-reduced molecular species were normalized by the abundances of the remaining 2+ precursor ions.

The stability parameter λ was calculated as follows.

$$\gamma = \frac{(I_R/I_{2+})}{(I_{RH}/I_{2+H})}$$

where I_R and I_{RH} are the intensities of the reduced species $[M + 2H]^{+\bullet}$ and I_{2+}, I_{2+H} are the parent ion intensities with subscript H again denoting the deuterated form.

Fig. 4A and B shows the plots of the parameters α, β, γ and λ for all stereoisomers in both solvents. The value $\lambda > 1.0$ indicates a higher stability of the reduced species than for the internal standard. Note that the λ values in the control experiment are above 1.0 for both solvents, indicating that the gas-phase stability of the reduced species of non-deuterated all-L Trp-cage was slightly higher than that of the deuterated species. The effect was small ($\Delta\lambda = 0.04$ and 0.03 for AB and Q solvents, respectively), and may be due to statistical fluctuation or due to vibrational excitation of heavier species during isolation in the gas-phase. The possibility of the influence of deuteration on the stability of reduced species in contrast to non-deuterated species is currently under investigation. Yet another possibility is

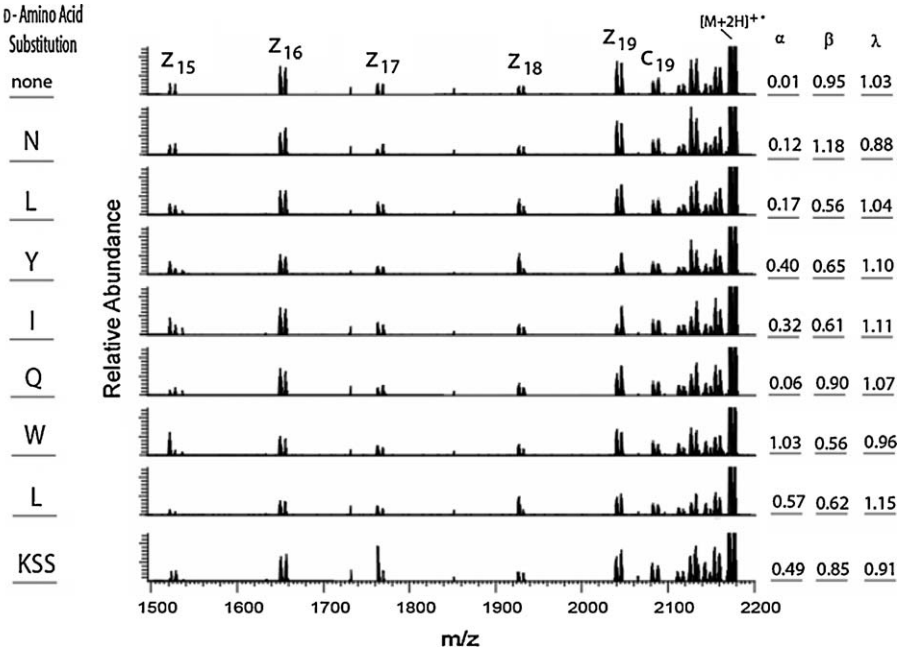

Fig. 3. Electron capture dissociation mass spectra of 2+ molecular ions produced by electrospray from 100 μM quinhydrone solution. α Reflects for D-substituted stereoisomers the deviation of their fragmentation pattern from that of the admixed internal standard (deuterated native form), β is a measure of structural disorder, and λ is a stability of the charge-reduced species, as described in the text.

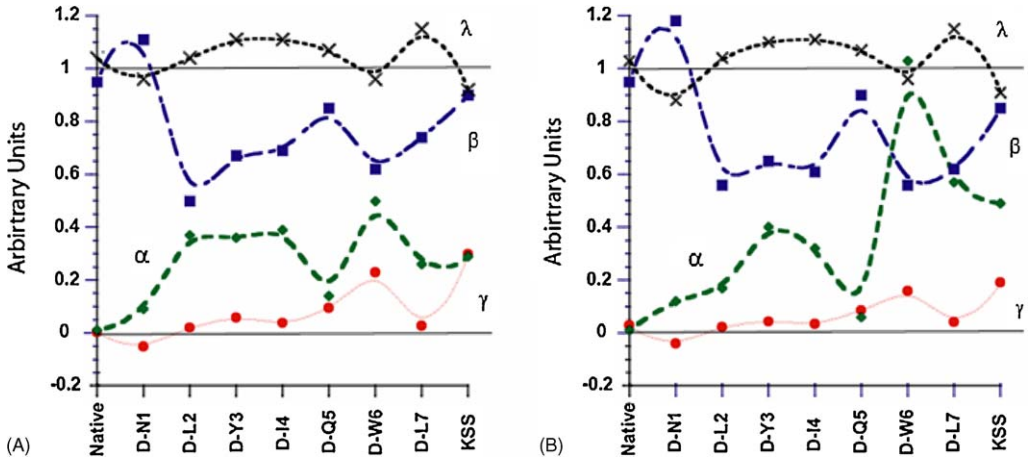

Fig. 4. Parameters α, β, γ and λ plotted as a function of D-amino acid substitution for (A) ammonium bicarbonate and (B) quinhydrone solutions. The meaning of the parameters is given in the text.

the already-mentioned slight racemization during the synthesis of deuterated Trp-cage.

The parameter α was defined as the standard deviation from the average value of the abundances of five z-ions normalized by those of the internal standard. In effect, α characterizes the likeness of the ECD fragmentation pattern to that of the all-L stereoisomer, with a value of zero being a perfect similarity. Not surprisingly, the D-substitution of the first two amino acids had a small effect on the ECD pattern and thus on the parameter α. Other α values are considered in Section 3.

The parameter α has disadvantages of being unidirectional (always positive) and measured relative to the ECD pattern of the all-L form. We also introduced a more general parameter β, which is the measure of *absolute* deviation of the abundances within a z-series from their own average value. More specifically, β is calculated as the standard deviation of z_{15}–z_{19} (S.D. z_{15}–z_{19}) divided by the average of the same z_{15}–z_{19} fragment ion series. The interpretation of β is the following. If the stereoisomer dication has no defined structure in the gas-phase, the population of ions is a complex mixture of inter-converting conformations, and its ECD pattern is the average of ECD patterns of the latter. The less structure there is, the more complex is the mixture of various conformations, and the more statistical becomes the ECD pattern, which for extremely complex mixtures should tend toward equal abundances for all z ions. Equal z-ion abundances (total disorder) result in small β values, while large β should indicate the presence of a defined structure.

For each ECD mass spectrum, the β values were calculated for the admixed stereoisomer and the internal standard separately. The latter values were all within a 0.93–0.98 interval (average value 0.95; standard deviation 0.02), showing good stability and repeatability of the experiment. Still, to minimize the influence of small variations between the experiments, β values for the admixtures were normalized by corresponding values for the internal standard. Control experiments for both solutions showed $\beta < 1.0$ for non-deuterated all-L isoform (somewhat less structured than the standard), which again may be a statistical fluctuation. Only one mutant showed $\beta > 1$, not surprisingly it was D-*Asn*^{1}. All other mutants turned out to be less structured in the gas-phase, again in parallel to the solution-phase. There was a good (anti)-correlation between β and α values ($r = -0.82$ and -0.58 for AB and Q, respectively), signifying that both α and β, despite the difference in their derivation, essentially capture identical features of MS/MS spectra.

2.4. Molecular modeling of Trp-cage chiral variants

To save computational time, five stereoisomers were selected for molecular dynamics simulations (MDS), four of which were present in the previous study [36]. The selected dications were of the all-L isomer and the stereoisomers that showed extreme values of one of the parameters or other noteworthy properties: D-*Tyr*^{3} (destabilization of the N-terminal α-helix), D-*Gln*^{5} (charged in the gas-phase; anomalously low α value), D-*Trp*^{6} (the most important residue for solution-phase structure; extreme α and β values) and D-*Leu*^{7} (extreme λ value; abnormally low γ value) mutants. Fig. 5 displays superimposed minimum-energy structures of the five simulated stereoisomers, the highlighted areas representing the protonated *Gln*^{5} and *Arg*^{16} residues. The obtained structures for all five stereoisomers were similar within 3 Å, and deviated from the "native" structure of the solution-phase all-L form by on average 4.0 Å. Some of the essential elements of the native conformation were preserved, such as the compact form with both termini in proximity to each other. However, the number of hydrogen bonds has increased almost two-fold, as was expected for the gas-phase. As a consequence of that and the disappearance of hydrophobic interactions, the overall shape became more elongated. The hydrogen bonding between the ε-hydrogen of the Trp side chain and the backbone amide is lost in all isomers.

The general impression from the gas-phase structures is that of a distorted but recognizable native conformation. The distance between the two charges in the simulated structures was 14.97 Å for all-L, 13.83 Å for D-*Tyr*^{3}, 13.17 Å for D-*Gln*^{5}, 15.42 Å for D-*Trp*^{6} and 12.17 Å for D-*Leu*^{7} mutants as measured using GROMACS.

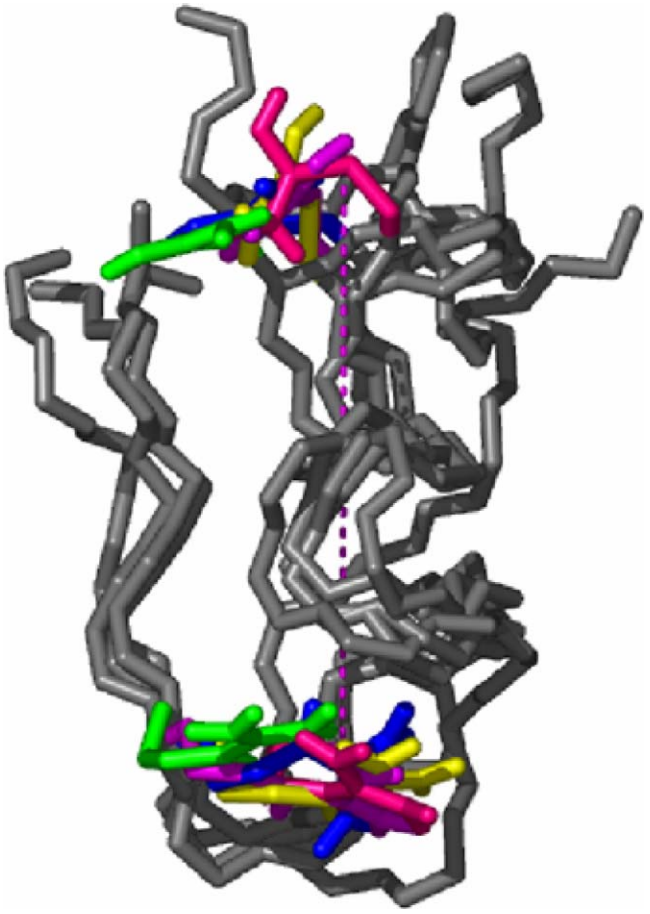

Fig. 5. Gas-phase structures of five Trp-cage stereoisomer dications produced by force-field molecular dynamics simulations: magenta, all-L; blue, D-*Tyr*^{3}; yellow, D-*Gln*^{5}; hot pink, D-*Trp*^{6}; green, D-*Leu*^{7}. PDB files can be found in Supplementary data for viewing.

3. Discussion

The primary goals of these studies were to provide insight into the following issues: (1) the conformational effects of single D-amino acid substitution as detected both in solution and the gas-phase; (2) viability of MS (CSD) and MS/MS (ECD) techniques to reflect slight structural alterations induced by a single D-amino acid substitution; (3) the degree to which gas-phase MS/MS and MDS data reflect structural changes detected by CD and CSD.

3.1. CD versus CSD

While the solution-phase CD measurements monitor the secondary structure effects with the emphasis on helical structure and to a lesser extent the tertiary structure, CSD assesses the overall deviation in compactness of the structure in reference to a control. Thus CD and CSD measurements are not directly comparable. However, within the same structural motif significant parallels can be observed. For instance, the small effect of D-*Asn*^{1} substitution on the α-helix and the dramatic effect of the D-*Tyr*^{3} substitution are obvious in both measurements. The D-*Leu*^{7} mutation gave a surprisingly small CSD shift ($\gamma = 0.03$–0.04), and showed a stable 3_1-helix in CD. CD found a random coil structure for D-*Tyr*^{3}, D-*Ile*^{4}, D-*Gln*^{5} and D-*Trp*^{6}. Of these four isomers, three showed large γ values, with a medium-range γ-value for D-*Ile*^{4}. Thus based on the low γ-values of the CSD measurements, prediction of the presence of a distinct solution-phase structure could be made for four stereoisomers (all-L, D-*Asn*^{1}, D-*Leu*^{2}, and D-*Leu*^{7}), all of which is in agreement with CD data. The only instance where CSD and CD partially disagreed is the tri-substitution D-$K^8S^{13}S^{14}$ that exhibited presence of 3_1-helical structure in CD and an unfolded structure in CSD. This discrepancy may reflect the inter-phase character of CSD measurements.

3.2. CD versus gas-phase MDS

Comparison of these two data sets is convenient as both relate to the secondary structure. The N-terminal α-helix detected with CD in solution is clearly discernable in the gas-phase structure of all-L isomer dications calculated by MDS. The D-*Tyr*^{3} mutation resulted in the random coil structure in CD; in MDS, disruption of the α-helix occurred in the first two residues.

To understand better the transition between the helical types upon D-substitution, the backbone carbonyl-to-amide hydrogen bonding networks in the helical part of the sequence of MDS-produced lowest-energy structures were analyzed in depth. Only bonds created by the first 11 carbonyls, before the proline disrupts the α-helix, were taken into account. The networks shown in Table 1 are strikingly non-random, with a tendency for helical structure shifts between the positions of the accepting carbonyls and donating amides. The number of functionalities, carbonyls or amides, that could contribute to an α-helix with the 3–4 residues shift from the carbonyl to the amide and a 3_1-helix with the shift of two residues were counted for each of the five simulated structures and the solution-phase structure. Fig. 6 shows the results of these calculations. The α-helical content in MDS structures is the highest for the native structures in both phases, and is the lowest for the D-*Leu*^{7} isomer. On the other hand, the latter isomer shows the highest 3_1-helical content, and it is the only one where the 3_1-helix surpasses the α-helix. In the three intermediate isomers, all motifs are present to a similar degree with the possible exception of the D-*Tyr*^{3} isomer which is slightly more 3_1-helical than the other two. These MDS results are in surprisingly good agreement with the CD data that gave clear α-helical structure for the native form and 3_1-helix for the D-*Leu*^{7} isomer, with the absence of a defined structure for other simulated isomers. This agreement reflects the basic similarity between the solution-phase and gas-phase structural features of Trp-cage.

3.3. CD versus MS/MS

The levels of structural detail probed by these two techniques are so different that only major features can be compared. A close look at MS/MS parameters α and β in Fig. 4 reveals that the major transition points occur upon chiral substitution of the residues L^2 and W^6. These changes reflect the two structural shifts identified by CD, the first one being α-helix to random

Table 1
Backbone amide and carbonyl hydrogen bonds, 1- all-L solution, 2- all-L vacuum, 3- D-Y^3, 4- D-Q^5, 5- D-W^6, 6- D-L^7

Amide											
	I^4	Q^5	W^6	L^7	K^8	D^9	G^{10}	G^{11}	P^{12}	S^{13}	S^{14}
Carbonyl											
N^1	1, 2, 4, 5	1, 2, 3, 4									
L^2	3	5, 6	1, 2, 6								
Y^3			3	1	6						
I^4				2, 3, 4	1						
Q^5					2						
W^6						1, 5		1			
L^7						6	1, 2, 3, 4, 5	2, 3, 4, 5			
K^8							6				
D^9											
G^{10}										1	
G^{11}											1

coil transition, and the second one the conversion of the random coil to partial 3_1-helix.

3.4. CSD versus MS/MS

The effect of D-substitution on conformational unfolding compared to the control as measured by CSD (parameter γ) ranks as follows: D-*Asn*^{1}, D-*Leu*^{2} ⟩ D-*Ile*^{4}, D-*Leu*^{7}, ⟩D-*Tyr*^{3} ⟩ D-*Gln*^{5} ⟩ D-$K^8S^{13}S^{14}$, D-*Trp*^{6} (Fig. 2A and B). In ECD of dications, the magnitudes of deviation from the control ECD pattern (parameter α) ranks as D-*Asn*^{1}, D-*Leu*^{2}, D-*Gln*^{5} ⟩ D-*Tyr*^{3}, D-*Ile*^{4} ⟩ D-*Leu*^{7}, D-$K^8S^{13}S^{14}$ ⟩ D-*Trp*^{6} (Fig. 4A and B), i.e., with many similarities with the CSD ranking. The biggest discrepancy was found between the rankings of D-*Gln*^{5}. The small α value for that residue is backed up by MDS which found that the structure of the all-L and D-*Gln*^{5} dications are extremely similar, with the average deviation of just 0.7 Å [36]. This has been a surprising finding, as the Q^5 amino acid is protonated in the gas-phase, and the difference in charge solvation patterns of L-*Gln*^{5} and D-*Gln*^{5} side chains could have been expected to result in different overall structures. The enhanced sensitivity of the solution structure to chiral inversion of *Gln*^{5} can be explained by the proximity of that residue to the all-important W^6 site.

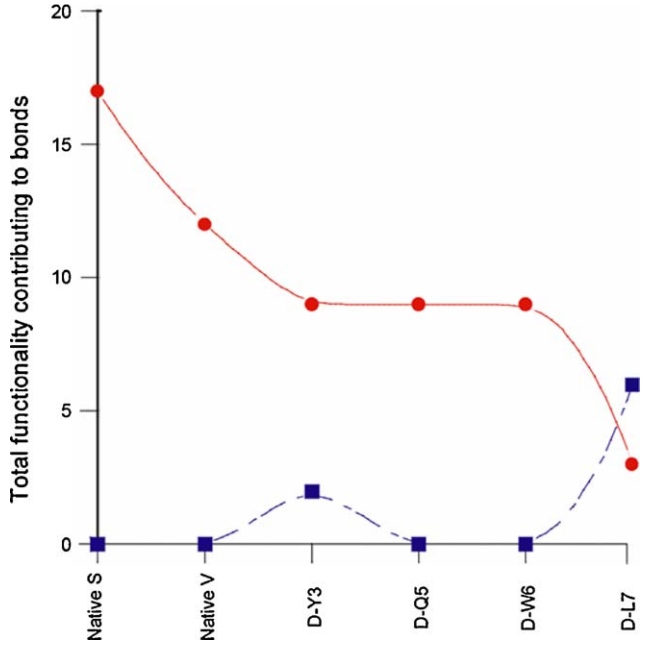

Fig. 6. Number of backbone functionalities (carbonyls and amides) involved in hydrogen bonding typical for helical structures in the native solution-phase structure (Native S) and minimum-energy structures calculated by MDS for five stereoisomer dications: all-L (Native V), D-*Tyr*^{3}, D-*Gln*^{5}, D-*Trp*^{6} and D-*Leu*^{7}. Round circles: α-helix; filled squares: 3_1-helix.

The overall correlation between α and γ values was $r = 0.47$ and 0.62 for AB and Q solvents, respectively. This correlation is statistically significant for $N = 9$ points of comparison, which confirms again that some coarse solution-phase features are preserved in the gas-phase.

The parameter β that presumably reflects the degree of variability among the gas-phase conformations of a given stereoisomer singled out the D-*Asn*^{1} mutant as the least disordered, followed by the all-L variant (Fig. 4A and B). These findings are in agreement with the solution-phase data. Understandably, D-*Gln*^{5} whose gas-phase structure is very similar to that of all-L was also among the less disordered mutants. A good agreement with the solution-phase CD findings was also the low degree of disorder for the triple D-substitution. At the same time, the most disordered was expectantly D-*Trp*^{6}. The only disagreements with the solution data were the low β values for the D-*Leu*^{2} and D-*Leu*^{7} isomers. This may be because the hydrophobic environment of vacuum enhances the impact of the chiral inversion of hydrophobic residues compared to the solution-phase. Consistent with that suggestion, the effect of chiral inversion of I^4 on β was also rather high.

3.5. MS/MS versus MDS

At first, the fact that most of the mutants showed a higher probability of $[M+H]^{\bullet}$ detection to that of the control ($\lambda > 1.0$) is surprising given that the solution-phase structures of these mutants are less compact. One should however remember that the stability of the reduced species is not the same as that of the precursor ions, and is mostly determined by the magnitude of the released recombination energy (RE). Immediately after

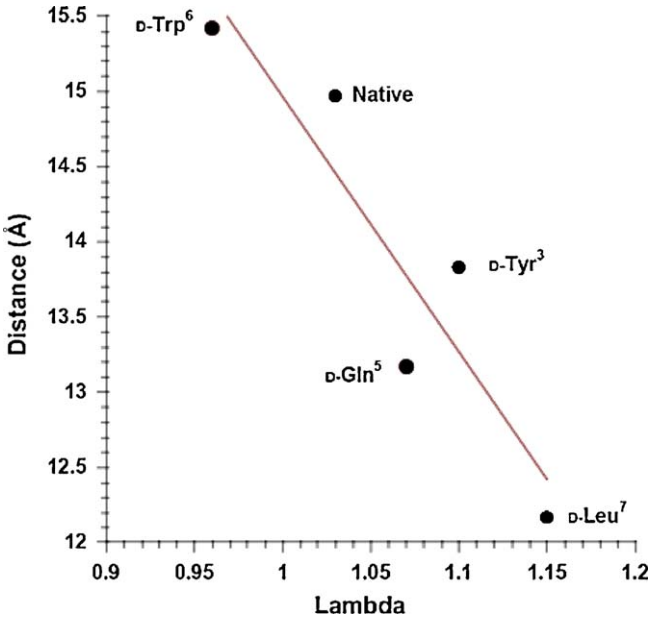

Fig. 7. MDS-determined distances between the charges located on the side chains of the residues *Gln*[5] and *Arg*[16] of the Trp-cage structures shown in Fig. 5 plotted against the parameter λ reflecting the stability of the charge-reduced species in ECD.

electron capture and facile N–C_α bond cleavage, the structure of charge-reduced $1+^\bullet$ radical molecular cations remains largely the same as of the precursor dications. Depending upon the balance between the RE value and the strength of *intra*-molecular hydrogen bonding, these radicals can either dissociate into *c* and *z* ions, or remain intact. The RE release depends in turn upon the potential columbic energy between the charged residues in the precursor dications, which is greater for conformations with proximal charges. As the number of hydrogen bonds is approximately the same for all stereoisomers, λ may be probing the proximity of the charges in the gas-phase precursor dications. To test this hypothesis, the ECD-derived λ values were plotted against the MDS-derived inter-charge distances (Fig. 7). A good correlation found ($r = 0.92$) strongly supports the hypothesis, and provides additional validity for the force-field simulation results. The slope of the obtained linear dependence can be used in further studies to predict inter-charge distances from ECD results. Note that inter-charge distance is a long-range constraint, e.g., in Trp-cage it relates to relative positions of the protonated residues 5 and 16.

4. Conclusions

The current study confirmed that conformational effects as subtle as that of a single D-amino acid substitution can be detected both in solution and the gas-phase by spectroscopic and mass spectrometry methods. The charge–state distribution measurements were found to reflect mostly the overall compactness of the molecules in solution, and to a lesser extent reflected their specific gas-phase properties. MDS results were fully consistent with the MS/MS results and provided an important link to such a long-range structural constraint as inter-charge distance. MDS also offered insight into the emergence of 3_1-helix from the a-helical precursor. Overall, strong parallels were found between the structure of Trp-cage mutants in solution and vacuum, firmly rejecting the inside-out conformation as a gas-phase structure of this molecule. The effect of L → D conversion of the critical Y^3 and W^6 residues was similar in both phases. The main differences were in the magnitude of the effect of chirality conversion of polar residues, e.g., Q^5 (stronger in solution) and non-polar residues, e.g., leucines 2 and 7 and isoleucine 5 (stronger in the gas-phase).

5. Materials and methods

Tryptophan cage protein, including the all-L form as well as the D-substituted variants, were synthesized in house using solid-phase Fmoc chemistry with an Intavis ResPep (Gladbach, Germany) automatic peptide synthesizer. D-Isomers of amino acids were purchased from Novabiochem (Laufelfingen, Switzerland) and Cambridge Research Biochemicals (Cleveland, UK). Peptides were purified after synthesis by reversed phase HPLC using a Vydac C18 column (Hesperia, CA).

Circular dichroism experiments were done using a JASCO J-715 spectropolarimeter with an automated PTC-343 temperature controller. All far UV samples were run at a 50 μM protein concentration in 200 μM pH 6.4 sodium phosphate buffer. The spectral range was between 185 and 250 nm with a 2 nm bandwidth and 0.2 nm data pitch; 1 mm cell was used with 8 s response. Five spectra were accumulated and summed. Near UV was done in the same buffer and on the same instrument but at a protein concentration of 1 mM, and a spectral range of 235–320 nM.

Mass spectrometry was performed using a 7 T LTQ FT mass spectrometer (Thermo, Bremen, Germany). Peptides were dissolved in either 2 mM ammonium bicarbonate containing 10% methanol or 100 μM quinhydrone (Sigma, Sweden), to a concentration of approximately 5 pmol/μL. Peptides were electrosprayed by direct infusion using a Proxeon nanoESI source (Odense, Denmark) with applied voltages ranging from 1100 to 1500 V. To eliminate the influence of the ESI sprayer, the same nanospray pulled glass capillary was used in each series of experiments, rinsing with ESI solvent between experiments.

ECD with LTQ FT was done as previously described [42]. Electrons were produced using a commercially available indirectly heated cathode provided by Thermo, an irradiation time of approximately 70 ms with an electron energy less than 1 eV.

In molecular dynamics simulations, GROMACS program package was used. All simulations were performed in vacuum using OPLS-AA force-field and the replica exchange approach, at 16 different temperatures from 275 to 419 K. Each simulation started from the "native" solution-phase structure determined by NMR, and lasted for 200 ns. Prior to the replica exchange run, an energy minimization was performed. To save the simulation time, the program assumed constant length of all covalent bonds. Analyses of H bonds were done using the GROMOS96 program g_hbond. The position of the ionizing proton on *Gln*[5] (side chain carbonyl oxygen) was determined by *ab initio* Gaussian proton affinity calculations. The minimum-energy structures for each

simulated stereoisomers were determined as described in Ref. [36].

Acknowledgements

Some of the Trp-cage stereoisomers used in this work were synthesized and purified by Å. Engström; others peptides were due to Marina Zoubareva. This work was supported by the Knut and Alice Wallenberg Foundation and Wallenberg Consortium North (grant WCN2003-UU/SLU-009 to RZ) as well as Swedish research council (grants 621-2004-4897 and 621-2003-4877 to RZ).

Appendix A. Supplementary data

Supplementary data associated with this article can be found, in the online version, at doi:10.1016/j.ijms.2006.04.012.

References

[1] M.R. Eftink, Energ. Biol. Macromol. 259 (1995) 487.
[2] N.J. Greenfield, Trac-Trends Anal. Chem. 18 (1999) 236.
[3] N.J. Greenfield, Anal. Biochem. 235 (1996) 1.
[4] N. Sreerama, M.C. Manning, M.E. Powers, J.X. Zhang, D.P. Goldenberg, R.W. Woody, Biochem. 38 (33) (1999) 10814.
[5] J.B. Fenn, M. Mann, S.F.W. Chin Kai Meng, C.M. Whitehouse, Science 246 (1989) 64.
[6] K.B. Shelimov, D.E. Clemmer, R.R. Hudgins, M.F. Jarrold, J. Am. Chem. Soc. 119 (1997) 2240.
[7] S.L. Bernstein, T. Wyttenbach, A. Baumketnert, J.E. Shea, G. Bitan, D.B. Teplow, M.T. Bowers, J. Am. Chem. Soc. 127 (2005) 2075.
[8] J.C. Jurchen, E.R. Williams, J. Am. Chem. Soc. 125 (2003) 2817.
[9] F.W. McLafferty, Z.Q. Guan, U. Haupts, T.D. Wood, N.L. Kelleher, J. Am. Chem. Soc. 120 (1998) 4732.
[10] K. Breuker, H.B. Oh, D.M. Horn, B.A. Cerda, F.W. McLafferty, J. Am. Chem. Soc. 124 (2002) 6407.
[11] P. Kebarle, J. Mass Spectrom. 35 (2000) 804.
[12] A.T. Lavarone, E.R. Williams, J. Am. Chem. Soc. 125 (2003) 2319.
[13] C.M. Adams, F. Kjeldsen, R.A. Zubarev, B.A. Budnik, K.F. Haselmann, J. Am. Soc. Mass Spectrom. 15 (2004) 1087.
[14] U.H. Verkerk, P. Kebarle, J. Am. Soc. Mass Spectrom. 16 (2005) 1325.
[15] L. Konermann, B.A. Collings, D.J. Douglas, Biochemistry 36 (1997) 5554.
[16] E.R. Badman, S. Myung, D.E. Clemmer, J. Am. Soc. Mass Spectrom. 16 (2005) 1493.
[17] K.B. Shelimov, M.F. Jarrold, J. Am. Chem. Soc. 119 (1997) 2987.
[18] T.J. Stevens, I.T. Arkin, Protein-Struct. Funct. Gen. 36 (1999) 135.
[19] S. Chowdhury, M.C. Lee, G.M. Xiong, Y. Duan, J. Mol. Biol. 327 (2003) 711.
[20] K. Breuker, F.W. McLafferty, Angew. Chem. Int. Ed. 44 (2005) 4911.
[21] L.L. Qiu, S.A. Pabit, A.E. Roitberg, S.J. Hagen, J. Am. Chem. Soc. 124 (2002) 12952.
[22] J.W. Neidigh, R.M. Fesinmeyer, N.H. Andersen, Nat. Struct. Biol. 9 (2002) 425.
[23] C.D. Snow, B. Zagrovic, V.S. Pande, J. Am. Chem. Soc. 124 (2002) 14548.
[24] A.T. Iavarone, J.H. Parks, J. Am. Chem. Soc. 127 (2005) 8606.
[25] D. Petrey, B. Honig, Protein Sci. 9 (2000) 2181.
[26] I.A. Kaltashov, S.J. Eyles, Mass Spectrom. Rev. 21 (2002) 37.
[27] F. McLafferty, Science 214 (1981) 280.
[28] F.W. McLafferty, Mass Spectrometry in the Analysis of Large Molecules, J. Wiley, New York, 1986, pp. 107.
[29] J.A. Loo, C.G. Edmonds, R.D. Smith, Science 248 (1990) 201.
[30] J.S. Brodbelt, Mass Spectrom. Rev. 16 (1997) 91.
[31] J.K. Hoerner, H. Xiao, A. Dobo, I.A. Kaltashov, J. Am. Chem. Soc. 126 (2004) 7709.
[32] R.A. Zubarev, N.L. Kelleher, F.W. McLafferty, J. Am. Chem. Soc. 120 (1998) 3265.
[33] R.A. Zubarev, D.M. Horn, E.K. Fridriksson, N.L. Kelleher, N.A. Kruger, M.A. Lewis, B.K. Carpenter, F.W. McLafferty, Anal. Chem. 72 (2000) 563.
[34] E.R. Badman, C.S. Hoaglund-Hyzer, D.E. Clemmer, J. Am. Soc. Mass Spectrom. 13 (2002) 719.
[35] C.M. Adams, R.A. Zubarev, Anal. Chem. 77 (2005) 4571.
[36] A. Patriksson, C. Adams, F. Kjeldsen, J. Raber, D. van der Spoel, R.A. Zubarev, Int. J. Mass Spectrom. 248 (2005) 124.
[37] L.J. Donald, D.J. Hosfield, S.L. Cuvelier, W. Ens, K.G. Standing, H.W. Duckworth, Protein Sci. 10 (2001) 1370.
[38] D. Lemaire, G. Marie, L. Serani, O. Laprevote, Anal. Chem. 73 (2001) 1699.
[39] C. Zhao, T.D. Wood, S. Bruckenstein, J. Am. Soc. Mass Spectrom. 16 (2005) 409.
[40] I.A. Kaltashov, A. Mohimen, Anal. Chem. 77 (2005) 5370.
[41] B.A. Barua, N.H, Lett. Peptide Sci. 8 (2001) 221.
[42] F. Kjeldsen, K.F. Haselmann, B.A. Budnik, E.S. Sorensen, R.A. Zubarev, Anal. Chem. 75 (2003) 2355.